Human Molecular Genetics, 2008, Vol. 17, No. 17 **2622–2632**
doi:10.1093/hmg/ddn162
Advance Access published on May 28, 2008

RNAi-mediated knockdown of dystrophin expression in adult mice does not lead to overt muscular dystrophy pathology

Mohammad M. Ghahramani Seno[1,2], Ian R. Graham[1], Takis Athanasopoulos[1], Capucine Trollet[1], Marita Pohlschmidt[1,†], Mark R. Crompton[1,‡] and George Dickson[1,*]

[1]School of Biological Sciences, Royal Holloway – University of London, Egham TW20 0EX, UK and [2]The Centre for Applied Genomics, Hospital for Sick Children, Toronto, Canada M5G 1L7

Received April 2, 2008; Revised May 16, 2008; Accepted May 23, 2008

Duchenne muscular dystrophy (DMD) is a fatal muscle wasting disorder caused by mutations in the dystrophin gene. DMD has a complex and as yet incompletely defined molecular pathophysiology. The peak of the pathology attributed to dystrophin deficiency happens between 3 and 8 weeks of age in *mdx* mice, the animal model of DMD. Accordingly, we hypothesized that the pathology observed with dystrophin deficiency may be developmentally regulated. Initially, we demonstrated that profound small interfering RNA-mediated dystrophin knockdown could be achieved in mouse primary muscle cultures. The use of adeno-associated virus vectors to express short-hairpin RNAs targeting dystrophin in skeletal muscle *in vivo* yielded a potent and specific dystrophin knockdown, but only after ~5 months, indicating the very long half-life of dystrophin. Interestingly, and in contrast to what is observed in congenital dystrophin deficiency, long-term (~1 year) dystrophin knockdown in adult mice did not result, *per se*, in overt dystrophic pathology or upregulation of utrophin. This supports our hypothesis and suggests new pathophysiology of the disease. Furthermore, taking into account the rather long half-life of dystrophin, and the notion that the development of pathology is age-dependent, it indicates that a single gene therapy approach before the onset of pathology might convey a long-term cure for DMD.

INTRODUCTION

Duchenne muscular dystrophy (DMD) is a progressive and severe genetic muscle wasting disease, which occurs in 1 out of every 3500 male births world-wide (1). Affected boys exhibit delayed motor milestones, generally become wheelchair-bound by the age of 12 due to progressive loss of functional skeletal muscles, and succumb to life-threatening respiratory insufficiency and cardiomyopathy by the early 20s.

The gene for dystrophin is located on the X chromosome, and codes for several isoforms, many of which are expressed in a tissue-specific manner (2). DMD and related animal models such as the *mdx* mouse (3,4) are caused by mutations in the dystrophin gene, which result in the absence of the largest isoform (Dp427) from skeletal, cardiac and smooth muscles and the CNS (2,5). Dp427 has been shown to exhibit complex interactions with many other structural and signalling molecules at the sarcolemma, and its absence is associated with a diverse range of molecular and cellular disturbances (6–9). While studies on whole-animal and cell culture models of dystrophin deficiency have allowed significant progress in unravelling the molecular pathology underlying DMD, the precise pathophysiology remains poorly understood (10,11).

Since first being demonstrated in 2001 that small interfering RNAs (siRNA) are capable of inducing specific down-regulation of genes in mammalian cells (12), many researchers have successfully used this technique *in vitro* and *in vivo* to knock down different genes (13,14). RNA interference (RNAi) provides the opportunity to study the effect of

*To whom correspondence should be addressed at: School of Biological Sciences, Royal Holloway – University of London, Egham, TW20 0EX, UK. Tel: +44 1784443545; Fax: +44 1784414224; Email: g.dickson@rhul.ac.uk
†Present address: Muscular Dystrophy Campaign, 61 Southwark Street, London SE1 0HL, UK.
‡Present address: Educational Development Centre, Royal Holloway – University of London, Egham TW20 0EX, UK.

knocking down a gene under controllable conditions. Similarly, the structure and function of miRNAs, which are expressed naturally in short-hairpin forms and processed into functional inhibitory molecules by the cellular machinery (15), inspired biologists to develop inhibitory vectors expressing short hairpins to target genes of interest (16,17). So far, this technique has successfully been exploited to target many genes specifically, including those in muscle cell cultures and skeletal muscles (18,19), as well as the dystrophin gene in Zebra fish (20).

In this study, we report the first demonstration of RNAi-mediated knockdown of Dp427 in primary cultures of skeletal muscle. Targeting of the Dp427 mRNA by siRNAs is very potent, stable and specific, and does not affect the expression of utrophin, a protein structurally very similar to Dp427 (21), nor of β-dystroglycan, which interacts directly with Dp427 (22). Our studies indicate that RNAi-mediated knockdown is a valuable experimental tool for induction and evaluation of dystrophin deficiency in a cell autonomous manner and under controllable conditions. Therefore, it opens windows to new experimental approaches in addressing the disease.

On the basis of the histology evidence that the pathology attributed to dystrophin deficiency is at its peak at a certain age (3–8 weeks) in *mdx* mice (23), it was proposed that dystrophinopathy may be developmentally regulated. Accordingly, we hypothesized that different patterns of pathology may be observed if dystrophin deficiency is introduced to the muscles of older mice. Moreover, on the basis of a report showing a rather long half-life for dystrophin expressed from a transgene in *mdx* mice (24), such a long half-life, which is important for gene therapy approaches, can also be expected from naturally occurring dystrophin. Therefore, taking advantage of high transduction efficiencies of AAV6 in skeletal muscles (25), we planned *in vivo* RNAi in skeletal muscles to evaluate our hypotheses. Tibialis anterior (TA) muscles of 1-month-old mice were transduced with recombinant adeno-associated virus pseudotype 2/6 (rAAV2/6) expressing a short hairpins targeting dystrophin (rAAVshDys) or one targeting firefly luciferase (rAAVshGL2) as a control.

In accordance with previous reports (25), high transduction levels (indicated by GFP expressed from the same vector) were observed in the treated muscles. However, the first signs of dystrophin reduction were only observed at around 9 weeks after transduction, as detected by immunostaining. Surprisingly, no obvious specific histopathology was observed in treated muscles even 13 months after transduction, while dystrophin had potently and specifically been knocked down during this period. Moreover, in contrast to what is observed in dystrophic muscles (26–28), no upregulation of utrophin was observed in this model of dystrophin deficiency.

RESULTS

Expression patterns of dystrophin (Dp427) and dystrophin-associated proteins in primary muscle cultures

In order to study the expression patterns of Dp427, β-dystroglycan (a dystrophin-associated protein) (22) and utrophin (a dystrophin-related protein) (21,27) in muscle primary cultures, an expression time-course study was conducted. This provided us with a starting point for planning siRNA experiments targeting Dp427 in muscle cultures. Primary muscle cultures were established using limb muscles of normal (C57Bl/10) and dystrophic (*mdx*) neonatal mice. The medium in the cultures was changed to induce differentiation 5 days after seeding. Cultures were harvested on days 2, 5, 7 and 10 for analysis of Dp427, β-dystroglycan and utrophin proteins by SDS–PAGE and western blotting. Dp427 was detectable at low levels in cultures derived from normal muscles at day 5, but was highly expressed at days 7 and 10 (Fig. 1A). Conversely, Dp427 was not detected at any stage in preparations from *mdx* muscle (Fig. 1A). Utrophin (Fig. 1B) and β-dystroglycan (Fig. 1C) were both detected in preparations from normal and dystrophic muscles at similar levels at all time-points analysed.

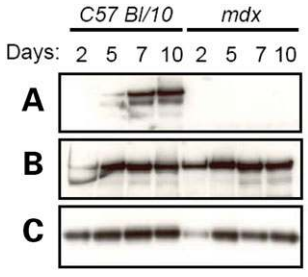

Figure 1. Expression patterns of Dp427, utrophin and β-dystroglycan in primary muscle cultures before and after differentiation. Cell cultures were prepared from normal (C57Bl/10) and dystrophin-deficient (*mdx*) mice, and western analysis performed on total protein extracts prepared on the subsequent days as indicated. Dystrophin (**A**) is not expressed in either undifferentiated (day 2) or differentiated dystrophin deficient cells (*mdx*), while it is expressed in normal differentiated (day >5) cells. Utrophin (**B**) and β-dystroglycan (**C**) are expressed at all stages in both strains.

RNAi-mediated knockdown of Dp427 in primary cultures of mouse muscle

Four different siRNAs (D1 to D4) were used to conduct dystrophin RNAi in primary muscle cultures from C57Bl/10 mice (Table 1). D1 is targeted to the region of Dp427 mRNA that codes for the N-terminus of the protein (see Table 1 for details of target region). D2 and D3 siRNAs target sequences common to the open reading frames of Dp427 and Dp71 (a short, non-muscle isoform of dystrophin) (29) to the 3′ side of exon 63. This sequence is conserved in human, mouse and dog. The target for D4 is situated in the 3′-UTR of Dp427 mRNA. This would also target Dp71 mRNA provided these two isoforms share a common 3′-UTR. A validated siRNA targeting firefly (*Photinus pyralis*) GL2 luciferase was also used as a non-specific control (12).

Primary cultures were established and siRNA transfections were performed at 100 nM on days 2 and 4 post-seeding. A single transfection on day 2 or 4 only has previously been demonstrated to be less effective in this system (M.M.G.S., unpublished data). Whereas GL2 siRNA had no effect on dystrophin expression (Fig. 2A, lanes 5 and 6), dystrophin siRNAs D1 (lanes 7 and 8) and D2 (lanes 9 and 10) specifically and potently downregulated Dp427. Similar results were also obtained with D3 and D4 (data not shown).

Table 1. Sequences and target positions of siRNAs targeting Dp427 transcript

siRNA	Sense strand (5′ > 3′)	Antisense strand (5′ > 3′)	Target position[a]
D1	GGCCUUACAGGGCAAAAACtt	GUUUUUGCCCUGUAAGGCCtt	386–404 Exons: 3–4
D2	GGCUAGCAGAAAUGGAAAAtt	UUUUCCAUUUCUGCUAGCCtg	10 527–10 545 Exons: 72–73
D3	GGAAGAAAACAGGAAUCUGtt	CAGAUUCCUGUUUUCUUCCtc	10 741–10 759 Exons: 74–75
D4	GGAUUUGUUUUCACCAAGAtt	UCUUGGUGAAAACAAAUCCtt	13 313–13 331 3′-UTR

[a]The target position in nucleotides from the 5′ end of the transcript for Dp427.

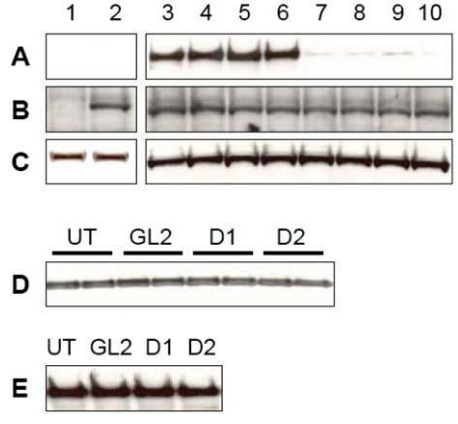

Figure 2. Dp427 is specifically and potently knocked down in mouse primary muscle cultures by the action of siRNAs. Western blot analysis was performed on protein extracts prepared following transfection of primary muscle cultures prepared from C57Bl/10 mice with siRNAs D1 (**A,** lanes 7 and 8) or D2 (lanes 9 and 10). This demonstrates down-regulation of Dp427, compared with untreated cells (lanes 3 and 4) or cells treated with a non-specific siRNA targeting firefly GL2 luciferase (lanes 5 and 6). However, Dp71 expression levels (**B**) do not show any change by siRNA treatments. Cell cultures from *mdx* mice, which do not express Dp427 (**A,** lane 2) but express Dp71 (**B,** lane2), and from GL105 mice that express neither (**A** and **B,** lane 1), were prepared and run in parallel. Equal amounts of quantified protein extracts were loaded onto the gels, as demonstrated by the use of an antibody to Nedd-4 as a loading control (**C**). Western blotting was also performed for the expression levels of β-dystroglycan (**D**), and of utrophin, (**E**). D1 and D2: C57Bl/10 muscle cell cultures treated with siRNA targeting dystrophin. GL2: C57Bl/10 muscle cell cultures treated with a non-specific siRNA targeting firefly GL2 luciferase. UT, untreated muscle cell cultures from C57Bl/10. Similar results were obtained with siRNAs D3 and D4 (data not shown).

Significant knockdown of Dp427 persisted for at least 6 days after the second siRNA transfection, the latest time-point evaluated (data not shown). None of the siRNAs tested had any detectable impact on the level of Dp71 (Fig. 2B; see Discussion). The same western blot membranes used to evaluate dystrophin status were also probed for Nedd-4 (a protein of ca. 90 kDa) as an internal loading control (Fig. 2C). Nedd-4 was chosen because its expression level does not seem to be affected by dystrophin deficiency (M.P., unpublished data). As additional comparative controls, samples were also analysed in parallel with culture lysates from the *mdx* mouse (Fig. 2A and B, lane 2), which expresses Dp71 but not Dp427, and from the GL105 ($Dmd^{mdx\text{-}\beta geo}$) mouse (30), which expresses neither (Fig. 2A and B, lane 1). All cell cultures and treatments were prepared at least in duplicates, and the results were also confirmed by independent replications.

In order to confirm the specificity of the dystrophin siRNAs in our system, lysates obtained from muscle primary cultures treated with dystrophin siRNAs were tested by western blotting using antibodies specific for utrophin and β-dystroglycan. Utrophin is structurally very similar to dystrophin (21), while β-dystroglycan is a component of the dystrophin-associated protein complex, and interacts directly with the C-terminus of dystrophin (22). The expression levels of both β-dystroglycan (Fig. 2D) and utrophin (Fig. 2E) are unaffected by treatment of the cells with siRNAs designed to target either dystrophin (lanes D1 and D2), or luciferase (lanes GL2), as compared with untreated cultures (lanes UT). As demonstrated in Figure 1, β-dystroglycan and utrophin are also expressed in primary muscle cultures prepared from dystrophic mice.

In order to confirm the loss of dystrophin from the sarcolemmal membrane, immunocytochemistry staining was performed on primary muscle cultures prepared from neonatal C57Bl/10 (Fig. 3A and B) and *mdx* mice (Fig. 3E and F), and on C57Bl/10 muscle cultures treated with the dystrophin siRNA D1 (Fig. 3C and D). Despite no detectable change in myotube morphology under phase-contrast microscopy (Fig. 3A, C and E), there is an almost complete lack of immunofluorescent staining arising from the use of a dystrophin-specific antibody in both *mdx* myotubes (Fig. 3F) and siRNA-treated C57Bl/10 myotubes (Fig. 3D), compared with strong immunostaining in untreated C57Bl/10 myotubes (Fig. 3B).

AAV2-based plasmid vectors express functional short hairpins

Transient-targeted oligonucleotide (siRNA) transfection *in vivo* is difficult and also demands repeated siRNA treatments to maintain desired downregulation of the gene of interest. However, it has been demonstrated that short hairpins expressed from expression vectors are processed into functional siRNAs by the cellular machinery and downregulate gene expression by the same pathway as that employed by synthetic siRNAs (16,17). Accordingly, in order to conduct dystrophin RNAi *in vivo*, an AAV-based construct was developed containing motifs expressing a short hairpin targeting Dp427 (shDys) or one targeting firefly GL2 luciferase (shGL2) as a control, under the influence of a modified cytomegalovirus (mCMV) promoter (see Materials and Methods and Supplementary Material, Fig. S1). The motif expressing shDys was designed based on the sequence of D2 siRNA, which targets a common sequence between Dp427 and Dp71 transcripts, conserved between human, dog and mouse. A CMV promoter driving expression of eGFP was also

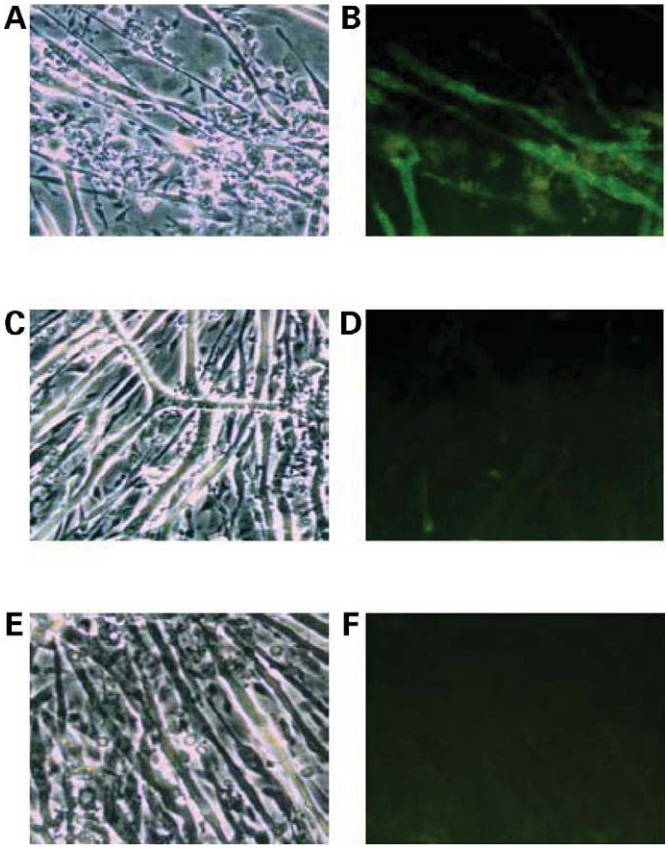

Figure 3. Dp427 is not expressed in myotubes in which dystrophin has been targeted by siRNAs. Primary muscle cultures prepared from C57Bl/10 mice were subjected to immunofluorescent staining using a primary antibody specific for dystrophin, demonstrating the presence of Dp427 at the sarcolemma after differentiation (**A** and **B**). Staining of C57Bl/10 muscle cells treated with siRNAs targeting dystrophin (**C** and **D**) and cell cultures from dystrophic *mdx* mice (**E** and **F**) revealed no dystrophin localized to the sarcolemma.

included in the final constructs. The construct expressing shDys (pAAVshDys-GFP) was tested for its ability to downregulate human dystrophin by co-transfection into 293T cells in conjunction with a plasmid expressing a full-length human dystrophin mRNA (pRSVhdys). This resulted in a substantial reduction in the level of dystrophin protein observed on western blots of extracts from cells treated with both plasmids (Fig. 4A, lanes 'shDys'), compared with those transfected with just pRSVhdys (Fig. 4A, lane 'hDy'). No reduction in dystrophin level was observed in extracts from cells co-transfected with pRSVhdys and pAAVshGL2-GFP (the construct expressing shGL2) (Fig. 4A, lanes 'GL2'). Similar results were observed by co-transfecting 293T cell with plasmids expressing dog dystrophin (pCicdys) and pAAVshDys-GFP (data not shown). Similarly, the plasmid expressing shGL2 (pAAVshGL2-GFP) was effective in downregulating over 60% of target expression level when co-transfected with pSpGL2 expressing GL2 luciferase (Fig. 4B). This indicates that both types of interfering plasmids are functional and thus suitable to be packaged into AAV particles for RNAi.

We have also observed that pAAVshDys-GFP is capable of demonstrating potent and specific downregulation of Dp427 in

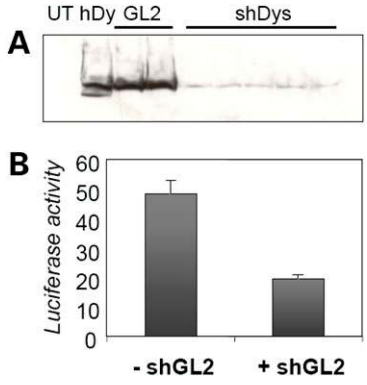

Figure 4. Efficiency of short hairpins expressed from plasmid vectors. Western blots on protein extracts obtained from 293T cells transfected with both pAAVshDys-GFP, which expresses a short-hairpin targeting Dp427, and pRSVhdys, expressing human dystrophin, demonstrate substantially reduced levels of Dp427 (**A,** 'shDys'), compared either with cells transfected with pRSVhdys alone (lane 'hDy'), or with cells co-transfected with control plasmid pAAVshGL2-GFP and pRSVhdys (GL2). UT, untransfected cells. The ability of the short hairpin expressed from pAAVshGL2-GFP to target firefly GL2 luciferase expressed from pSpGL2 is also demonstrated (**B**). pSpGL2 was transfected into 293T cells in the presence (+ shGL2) or absence (− shGL2) of pAAVshGL2-GFP and subsequently analysed for luciferase activity.

myofibres of TA muscles of C57Bl/10 mice transfected with this construct by electrotransfer (data not shown).

Dystrophin knockdown in adult mice does not lead to overt muscular dystrophy pathology

Approaches taken for plasmid delivery into skeletal muscle cells *in vivo* are aggressive and exert non-specific changes to the transfected cells. For instance, as also observed in our experiment of targeting dystrophin in muscles by electrotransfer of plasmids expressing short hairpins, many centrally nucleated myofibres indicative of regeneration could be observed in the treated muscles (data not shown). This may change the expression pattern of many proteins including dystrophin. To avoid this, and due to the much better long-term expression of AAV *in vivo*, rAAV2/6 vectors expressing short hairpins targeting dystrophin (rAAVshDys-GFP) or firefly luciferase (rAAVshGL2-GFP) as a control were propagated and used to study Dp427 knockdown in TA muscles in C57Bl/10 mice (see Materials and Methods for details). Tibialis anteriors of 1-month-old mice were injected directly with the viral vectors, and treated muscles were collected over a time-course following injection, starting at 9 days. Levels of GFP expression indicative of >90% transduction were observed both microscopically, in frozen sections of the treated muscle (Fig. 5A), and macroscopically (Fig. 5B), as has been seen in the previous reports (25). However, the first changes in the Dp427 expression levels at the sarcolemma were not detectable until 9 weeks after transduction, as evaluated by immunostaining (Fig. 6, 'shDys'). By Week 20, Dp427 was largely undetectable in TAs transduced with rAAVshDys-GFP, resembling the muscles of *mdx* mice (Fig. 6, '*mdx*'). Control TAs that had been transduced with rAAVshGL2-GFP were expressing similar levels of Dp427 to normal (Fig. 6, 'shGL2').

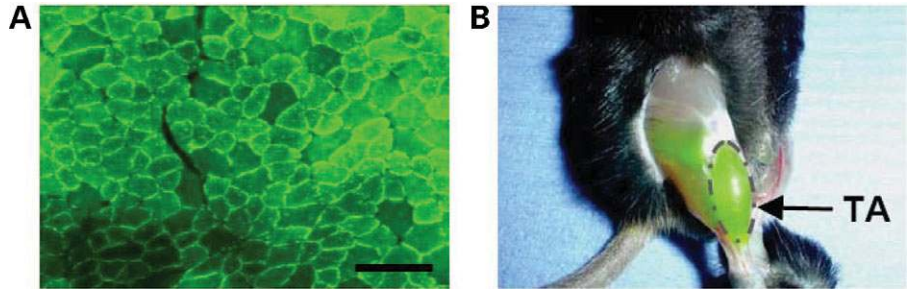

Figure 5. rAAV2/6 transduction of muscle cells. Tibialis anterior muscles of C57Bl/10 mice were injected with either rAAVshDys-GFP or rAAVshGL2-GFP, resulting in a high level of transduction detectable by GFP expression microscopically as early as 9 days after injection (**A**), and macroscopically by 2 weeks after injection (**B**). This high level of GFP expression was maintained throughout the 56 weeks of the experiment, indicative of the presence of functional expression cassettes in myofibres. The smearing of GFP expression observed on parts of the thigh muscles is due to the leakage of the injected solution containing the virus. Bar = 100 μm.

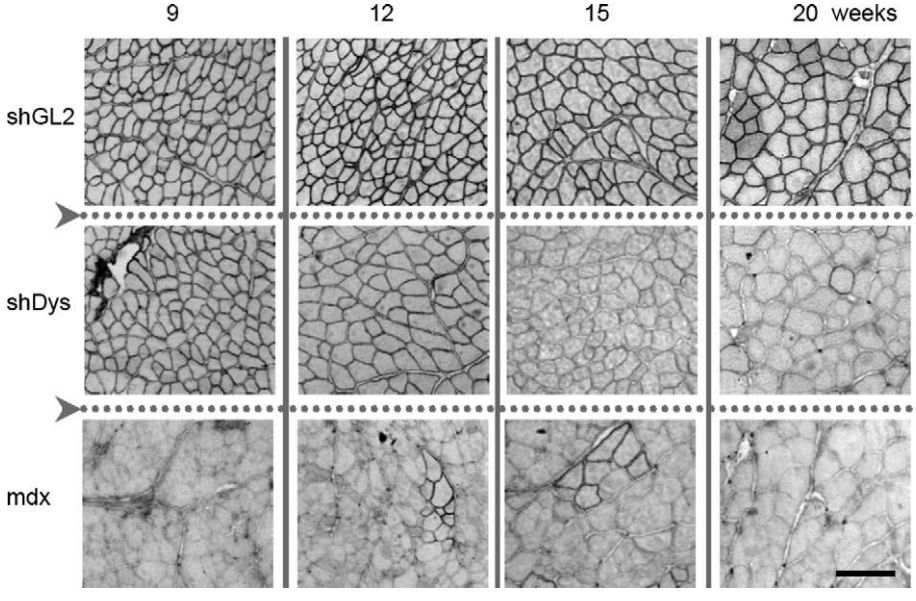

Figure 6. Time-course of Dp427 knockdown in TA muscles of C57Bl/10 mice in response to shRNAs. Tibialis anterior muscles of C57Bl/10 mice were injected with 2×10^9 vector genomes of rAAV2/6-shDys-GFP and harvested over a period of 20 weeks, as indicated. Immunohistochemical staining was performed for dystrophin on 10 μm muscle sections, showing a gradual reduction of dystrophin staining at the sarcolemma of TAs transduced with rAAVshDys-GFP (Panels 'shDys'). The level of dystrophin expression at 20 weeks after transduction made these treated muscles indistinguishable from TAs obtained from *mdx* mice (Panels '*mdx*'). The muscles treated by injection with rAAV2/6-GL2-GFP (Panels 'shGL2') did not show any changes in Dp427 expression at the sarcolemma, indicating the specificity of Dp427 knockdown by rAAVshDys-GFP. Bar = 100 μm.

To ensure identical immunostaining treatments were applied to different samples, muscles in which Dp427 had been knocked down using rAAVshDys-GFP and control muscles such as those treated with rAAVshGL2-GFP or *mdx* muscles were always mounted on a single slide and immunostained together (Supplementary Material, Fig. S2).

Interestingly, none of the histopathology characters observed in *mdx* muscles were observed in our model, even as long as 56 weeks after the transduction of TAs. At this stage, several centrally nucleated myofibres were observed, but these occurred in both control (12.8%) and experimental (10.7%) groups of TAs, with no statistically significant difference between them (Fig. 7A; $P = 0.592$). We also analysed the distribution of areas of individual fibres for each of the groups, and found no difference in the distribution for muscles treated with rAAVshDys-GFP or rAAVshGL2-GFP, but a statistical difference ($\chi^2 = 963$, $P < 0.001$) for muscles treated with rAAVshDys-GFP compared with *mdx* muscles (Fig. 7B).

In *mdx* mice, which lack Dp427 expression at the sarcolemma, the expression patterns of dystrophin-associated proteins such as dystroglycans and sarcoglycans as well as of utrophin are also altered (28). In the histological preparations of muscles in which dystrophin had been knocked down by RNAi, we did not observe the histopathology commonly seen in *mdx* muscles. To verify whether this difference can also be observed at the molecular level, the status of β-dystroglycan, α-sarcoglycan and utrophin was evaluated by immunostaining in our model of dystrophin deficiency 56 weeks after administration of the AAV vectors expressing short-hairpin RNA (shRNA) against dystrophin (Fig. 8, 'shDys') or luciferase (Fig. 8, 'shGL2'). Immunostaining

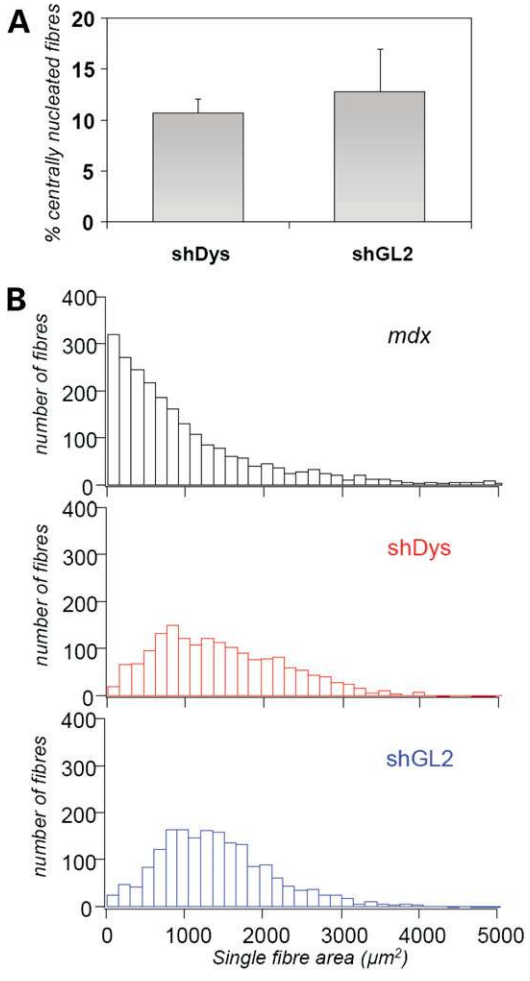

Figure 7. Analysis of fibre morphology in treated muscles. Frozen sections of TAs collected 56 weeks after transduction with rAAVshDys-GFP or rAAVshGL2-GFP were analysed for the number of fibres with centrally located nuclei (**A**), and for fibre diameter (**B**). The number of centrally nucleated fibres was not significantly different between muscles treated with rAAVshDys-GFP (Dys) and rAAVshGL2-GFP (GL2) [10.7% ($n = 3$, SEM = 1.4) versus 12.8% ($n = 3$, SEM = 4.2), respectively; *t*-test $P = 0.592$]. The single fibre area distribution (B) for muscles treated with rAAVshDys-GFP is statistically different from *mdx* muscle ($n = 3$, χ^2 test, $\chi^2 = 963$, $P < 0.001$), and indistinguishable from TAs treated with rAAVshGL2-GFP.

was also performed at 20, 24 and 32 weeks after virus administration (data not shown). Interestingly, despite the absence of histological changes, β-dystroglycan (Fig. 8, 'DG') and α-sarcoglycan (Fig. 8, 'SG') were found to be downregulated at all time points at the sarcolemma of TAs in which dystrophin had been knocked down, in common with findings in the *mdx* mouse; but, in contrast to skeletal muscles in *mdx* (Fig. 8, '*mdx*'), utrophin levels did not show any upregulation at the sarcolemma of these muscles (Fig. 8, 'Utr').

DISCUSSION

Duchenne muscular dystrophy and dystrophin-deficient animal models are characterized by the absence of a single protein as a primary molecular defect (5,31), yet the resulting molecular, cellular, tissue and whole-organism pathology is very complicated, due in part to the multi-functional nature of dystrophin itself and in part to physiological responses to myofibre necrosis (9–11). Therefore, despite the huge effort that has been put in to the study of the molecular basis of the disease, the physiopathology of this disorder is still not well-defined.

In the first part of this work, we demonstrate the susceptibility of Dp427 mRNA to be effectively targeted by siRNAs, thus making RNAi an attractive tool for studying the molecular pathology of DMD under controllable conditions. Four different siRNAs were tested in cultured muscle cells, showing high-level, sustained Dp427 knockdown. The best performing subject was then used to achieve long-term dystrophin knockdown when expressed as a short-hairpin RNA on an AAV vector. This gives an indication as to the stability of dystrophin protein, as well as an insight into the molecular pathology of the disease.

All four of the siRNAs used were shown to be very effective at reducing the levels of Dp427 in excess of 90% (Fig. 2 and data not shown). Intriguingly, three of these siRNAs (D2, D3 and D4) had been designed to target Dp71 mRNA as well as Dp427 mRNA. However, none of our experiments using these siRNAs showed any changes in Dp71 levels detectable by western blotting. Dp71 is expressed in myoblasts, but its expression is downregulated in differentiated myotubes (32). The persistence of Dp71 in differentiated primary muscle cultures may be explained by the presence of other cells, such as fibroblasts, within primary muscle cultures that are more refractory to transfection, but may express Dp71 (33). An additional, but not mutually-exclusive, explanation lies in the observation that dystrophin expressed from a transgene (24) and, as also shown in this work, the naturally expressed Dp427 both have a particularly long half-life. If this is also the case for Dp71, then its expression in myoblasts prior to transfection would result in a stable protein which would not diminish after a short exposure of its mRNA to siRNA.

In addition to demonstrating the functionality of the short-hairpin expressing vectors, the co-transfection of plasmid vectors expressing shRNAs and dystrophin also demonstrated an early expression of short hairpins. Due to the predicted long half-life of dystrophin (24), if short-hairpin expression from mCMV was limited, a higher background level of dystrophin protein in co-transfection experiments would have been expected. However, in these experiments, dystrophin expression in lysates obtained 3 days after co-transfecting 293T cells was close to zero, indicating a quick build up of short hairpins inside the cells (Fig. 4A). Nevertheless, this assumes a similar half-life for dystrophin in 293T cells and muscle cells.

By taking advantage of the high transduction efficiencies of AAV6 in skeletal muscle (25), and the specific capability of short hairpins expressed from vectors in directing RNAi (17), we were able to achieve a very specific, extensive, prolonged and powerful dystrophin knockdown in mouse skeletal muscle. The first signs of dystrophin reduction detected by immunostaining were noticed in muscles treated with rAAVshDys-GFP only 9 weeks after transduction (Fig. 6). The level of dystrophin further reduced as time progressed and was below the limit of detection at 20 weeks after injection.

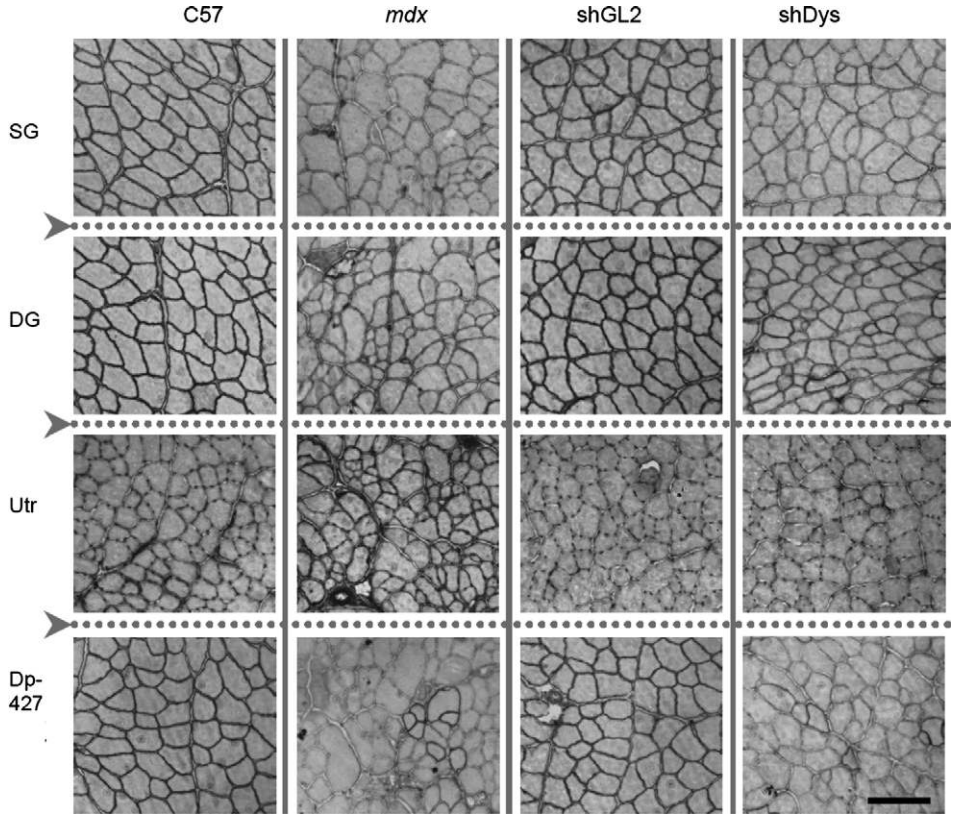

Figure 8. Molecular features of *mdx* muscles in TAs treated by dystrophin RNAi. Tibialis anterior muscles of C57Bl/10 mice were injected with 2×10^9 vector genomes of rAAV2/6-shDys-GFP (Column 'shDys') or rAAV2/6-shGL2-GFP (Column 'shGL2'), and harvested 56 weeks later. Immunohistochemical staining was performed on 10 μm muscle sections using antibodies specific for α-sarcoglycan (Row 'SG'), β-dystroglycan (Row 'DG'), utrophin (Row 'Utr') and dystrophin (Row 'Dp427'). Muscles from untreated C57Bl/10 mice and from dystrophin-deficient *mdx* are included for comparison. Similar features were also observed in muscles collected 20, 24 and 32 weeks after injection. Bar = 100 μm.

This suggests a long half-life for naturally expressed dystrophin in agreement with observations made by others in which dystrophin expressed from a tetracycline-responsive transactivator system could be detected at the sarcolemma of *mdx* muscles up to 26 weeks after they had repressed its expression (24). This long half-life of dystrophin is an advantage in gene therapy approaches for treatment of dystrophin deficiency.

However, interestingly and contrary to what has been observed previously in *mdx* mice (23,34,35), dystrophin knockdown in skeletal muscles (TAs) of adult mice was not accompanied by any obvious pathology.

The normal expression of dystrophin-associated proteins such as dystroglycans and sarcoglycans at the sarcolemma are deregulated by dystrophin deficiency in *mdx* mice (28). We have demonstrated here that β-dystroglycan and α-sarcoglycan are specifically downregulated at the sarcolemma in TAs treated with rAAVshDys-GFP (Fig. 8). Dystrophic muscles of *mdx* mice display an extensive and progressive degeneration followed by regeneration. Concomitant with this, the regenerating myofibres also express utrophin at the entire sarcolemma (26–28). Interestingly, in our model of dystrophin deficiency, despite downregulation of dystrophin, β-dystroglycan and α-sarcoglycan, and even after dystrophin had been subject to knockdown for over 1 year, neither the presence of degenerative myofibres nor the expression of utrophin at the sarcolemma was observed (Fig. 8).

It is believed that the upregulation of utrophin at the sarcolemma in the absence of dystrophin is due to the absence of competition between dystrophin and utrophin for common binding ligands (36). However, during the postnatal development of *mdx* muscles, utrophin is first downregulated before the third week of age, but is upregulated in regenerated myofibres after degeneration and necrosis starts at a later stage (37). There is also evidence of the positive influence of factors associated with the chronic inflammation seen in *mdx* mice on the stabilization and augmentation of extrasynaptic sarcolemmal utrophin (38). This could explain why in our system, in which there was no apparent inflammation, we did not detect any overexpression of utrophin at the sarcolemma.

In *mdx* mice, an acute process of degeneration and regeneration is observed between the ages of 3 and 8 weeks (23). We transduced the TAs when mice were 4 weeks old, and the first signs of dystrophin downregulation detectable by immunostaining were observed 9 weeks later, i.e. when mice were 13 weeks old. This age is well beyond that at which the associated pathology in *mdx* begins. One way in which this could be interpreted is that the pathology observed with dystrophin deficiency occurs via a developmentally regulated mechanism, and the absence of any pathology detectable by

H&E staining of histological preparations and by fibre size analysis in our model is due solely to targeting dystrophin at a different developmental stage. One potential opportunity for specifically testing this hypothesis would be to knock down dystrophin using this technique at an embryonic stage by, for example, creation of a transgenic mouse expressing a dystrophin-specific shRNA.

It has been suggested that accelerated growth rate in neonates may contribute to the extensive pathology observed in dystrophic muscles at this stage, and therefore that the molecular pathology observed in young affected individuals might be different in some aspects to that of the adult (39). Our work supports this hypothesis by demonstrating that dystrophin deficiency in muscles will be better tolerated if it is induced at stages when the muscle growth rate is slower.

Synapse elimination and maturation is one of the most important developmentally regulated phenomena happening at nearly the same age of mice, i.e. around 2–3 weeks, when overt pathology starts in skeletal muscles of *mdx* mice (40). Hence, it may be argued that the absence of dystrophin may result in the deregulation of pathways that ensure proper synapse elimination and maturation. In fact, it has been demonstrated that while the neuromuscular junction (NMJ) structure in *mdx* neonate is no different to that of normal muscles before the onset of the pathology, the process of synapse elimination and monoinnervation is enhanced in *mdx* mice at this stage (41). Synapse elimination is necessary for the formation of co-ordinated motor units. A motor unit refers to a group of myofibres innervated by one motor neuron, so the majority of these myofibres will undergo an action potential resulting in contraction by each stimulus received from the motor neuron innervating them. During the process of synapse elimination/maturation, the multineural innervation of each post-junctional membrane (PJM) changes to status in which only one axon is innervating each PJM. Moreover, the density of AChRs and ion channels such as sodium channels also increases in the PJM area, ensuring a proper response to each stimulus (42). Interestingly, it has recently been indicated that mutations of dys-1, a dystrophin homologue in *Caenorhabditis elegans*, may result in misregulation of potassium channels (SLO-1) (43). Moreover, it has been demonstrated that in dystrophic muscles, the half-life of adult type AChRs and the number of functional AChRs are less than normal (44–46). Therefore, it may be postulated that the establishment of coordinated motor units, i.e. formation of units where at least the majority of myofibres composing each unit will undergo a simultaneous action potential, may be adversely affected in the absence of dystrophin. Therefore, unsynchronized contractions of myofibres composing a dystrophic motor unit would exert high mechanical pressure on the contracting myofibres of the unit at each action, resulting in cell injury.

The necrosis and regeneration happening in adult *mdx* muscles induce changes to the organization of the NMJ and associated structures that may not be a direct consequence of dystrophin deficiency (41,47). Hence, studying the NMJ and associated structures in our model of dystrophin deficiency, which is not accompanied by necrosis and regeneration of myofibres, but is happening in adulthood, may be helpful in elucidating the pure effect of the dystrophin deficiency, void of regeneration-associated changes, on the development and organization of these structures.

Finally, localized absence of pathology may also be explained by the proposed supportive/protective role of dystrophin against mechanically induced injuries in skeletal muscles. We targeted dystrophin in a single muscle (TA) in the body; the myofibres which do not express dystrophin in this model may not be exposed to the usual pressures and forces they are in a dystrophic animal with general weakness. To address this, a more extensive dystrophin knockdown applied either locally in a whole limb or systemically to the whole body using AAVshRNA might be needed. Applying physical stress such as long- and/or short-term exercise to the muscle in which dystrophin has been downregulated would also be informative. Furthermore, it may also be helpful to apply eccentric muscle contractions to induce damage, for example, by electrical stimulation of stretching muscles to study the recovery process of the dystrophic muscle and compare it to that of congenital dystrophin deficiency in the adult.

Taken together, in addition to the establishment of a long half-life for naturally expressed dystrophin, we have produced a new dystrophic model using RNAi which opens new windows for studying the molecular pathology of dystrophic conditions.

MATERIALS AND METHODS

Cell culture and siRNA transfection

Primary muscle cultures were prepared from limb muscles of 3–5-day-old mice, as described previously (48). The cell preparation obtained from each animal was used to seed two 6-well plates. After 48 h, these primary muscle cultures consisted of a ~60% confluent monolayer of proliferating mono-nucleate cells and, at this point, were subjected to the first transfection treatment. Four siRNAs targeting dystrophin were tested (Table 1). These siRNAs were designed using an algorithm developed by Cenix BioScience GmbH (Dresden, Germany) and produced by Ambion (Austin, USA). Control siRNA-targeting firefly GL2 luciferase was obtained from Dharmacon (Lafayette, USA). siRNAs were introduced into the primary muscle cultures at a final transfection concentration of 100 nM using Oligofectamine (Invitrogen, Paisley, UK), following the manufacturer's instructions. Ninety-six hours after seeding, when cultures were fully confluent, culture medium was changed to serum-free Dulbecco's minimum essential medium (DMEM) to induce differentiation of myoblasts, and a second transfection was performed.

Antibodies

We used the following antibodies in our experiment: mouse monoclonal antibody NCL-DYS2 detecting the C-terminus of dystrophin (clone Dy8/6C5; Novocastra Laboratories, UK); mouse monoclonal antibody detecting the N-terminus of utrophin (clone DRP3/20C5, Vector Laboratories, UK); mouse monoclonal antibody NCL-b-DG detecting β-dystroglycan (clone 43DAG1/8D5, Novocastra Laboratories, UK); mouse monoclonal antibody NCL-a-SG detecting

α-sarcoglycan (clone Ad1/20A6, Novocastra Laboratories, UK); Nedd-4 mouse monoclonal antibody detecting Nedd-4 (Transduction Laboratories, USA) and HRP (horse radish peroxidase) - conjugated goat anti-mouse secondary antibody (Jackson ImmunoResearch Laboratories, USA).

Western blotting

Protein extracts were prepared in 200 μl/well lysis buffer containing 75 mM Tris–HCl (Sigma-Aldrich, UK), pH 6.8; 10% SDS (Sigma-Aldrich); 20% glycerol (Sigma-Aldrich); 200 mg/ml EDTA (Sigma-Aldrich) and 20 μg/ml phenylmethylsulfonyl fluoride (Sigma-Aldrich), and passed through a 25-gauge hypodermic needle several times to shear DNA and hence reduce viscosity. Dithiothreitol (Sigma-Aldrich) and bromophenol blue were excluded from the buffer in this stage as they interfered with protein assay. To determine the total protein amount in samples, the bicinchoninic acid (BCA) protein assay kit and protocol was used (Perbio Science, UK). Twenty micrograms of each of the samples were run on either Bis-Tris 4–12% NuPAGE gels (Invitrogen) using MES SDS running buffer (Invitrogen) for β-dystroglycan, or on Tris-Acetate 3–8% NuPAGE gels (Invitrogen) using Tris-acetate SDS running buffer (Invitrogen) for utrophin and dystrophin.

Immunofluorescence staining

Primary cultures were prepared, grown on Lab-Tek chamber slides (Nunc, Denmark) and treated as described earlier. Immunostaining was performed using the Vectastain ABC kit (Vector Laboratories) and fluorescein avidin D (Vector Laboratories), according to the manufacturer's protocol.

Construction of plasmids expressing short-hairpin RNAs

It has been shown that generally used CMV promoters do not express functional short hairpins (49,50). Accordingly, CMV has been modified to clone the short-hairpin expressing elements as close as possible to its transcription initiation site. For this project, the modified CMV (mCMV) was PCR-amplified from peGFP-N3 (Clontech, UK) using primers as had been described previously (51), but modified to include *Spe*I and *Xho*I restriction sites at the 5′ and 3′ ends of the amplified mCMV, respectively. The primers sequences were as follows: forward (GGACTAGTCAGA TCTTAGTTATTAATAGTAATCAATTACGG); reverse (CCGCTCGAGACGGTTCACTAAACCAG).

On the basis of the sequence of D2 siRNA, the sense (TCGAGGCTAGCAGAAATGGAAAATTCAAGAGATTTT CCATTTCTGCTAGCCTG) and antisense (AATTCAGGCT AGCAGAAATGGAAAATCTCTTGAATTTTCCATTTCTG CTAGCC) strands of shDys were designed, so that the annealed shDys would be directly ligated to *Xho*I and *Eco*RI restriction sites on the vector. Similarly, based on GL2 siRNA sequence, sense (TCGAGCGTACGCGGAATACTT CGATTCAAGAGATCGAAGTATTCCGCGTACGTTG) and antisense (AATTCAACGTACGCGGAATACTTCGATCTC TTGAATCGAAGTATTCCGCGTACGC) strands of shGL2 were also designed.

Sense (AATTCAAGCTTAATAAAGGATCCTTTATTTT CATTGGATCCGTGTGTTGGTTTTTTGTGTGCGGCCGC GA) and antisense (CGCGTCGCGGCCGCACACAAAAAA CCAACACACGGATCCAATGAAAATAAAGGATCCTTT ATTAAGCTTG) strands of the minimal polyA (mPolyA) were designed as described previously (51), but modified to include the restriction sites of *Eco*RI–*Hin*dII and *Mlu*I at the 5′ and 3′ ends of the annealed product, respectively. The mPolyA was designed so that it would maintain open sites for ligation, after sense and antisense strands are annealed.

pAdTrack (52), which had a CMV-eGFP fragment flanked by *Kpn*I and *Xba*I sites at 5′ and 3′ ends, respectively, was used to amplify the CMV-eGFP cassette using Templiphi 500 amplification kit and protocol (GE Healthcare, UK). The CMV-eGFP motif was then sequentially digested out of the rest of the amplified product to be selectively cloned into either pAAVshDys (Supplementary Material, Fig. S1) or pAAVshGL2.

All oligos were constructed by Proligo (UK). All motifs explained here were sequentially ligated into the multiple cloning site of pDD345 (a kind gift from Dr Dongsheng Duan, University of Iowa, USA) (Supplementary Material, Fig. S1) using FastLink DNA ligation kit (Epicentre, USA).

Luciferin detection assay

Genejuice transfection reagent (Novagen, UK) was used for transfection of plasmid constructs into 293T cells, according to the manufacturer's protocol. Forty-eight hours after co-transfection, cells were harvested to measure luciferase activity using Bright-Glo™ luciferase assay system (Promega, USA) according to the manufacturer's instructions, and the signals were measured using a DLReady Luminometer (DLReady, TD 20/20, Turner Design, UK). The experiment was performed in triplicates and was also independently replicated.

Propagation of rAAV

For the production of rAAV2/6 pseudotyped particles co-expressing shRNAs and eGFP, the method utilizing a two plasmid co-transfection system was used (53). AAV-based plasmids expressing short hairpins were co-transfected with pDP6r helper (a kind gift from J. Kleinschmidt, DKFZ, Heidelberg, Germany) into 293T cells grown in roller bottles using the calcium phosphate technique (54). Cell lysates were used to purify viral particles using Iodixanol step gradient ultracentrifugation techniques (55). Dot blot hybridization using an internal probe was used to determine the virus particles titres (56,57).

Animal husbandry

Animals were bred in-house and food and water provided *ad libitum*. They were maintained, and *in vivo* experimentation was conducted under statutory Home Office recommendation, regulatory, ethical and licensing procedures and under the Animals (Scientific Procedures) Act 1986 (PPL 70/6160).

rAAVshDNA-Gfp transduction of TAs of C57Bl/10 mice

Four-week-old C57Bl/10 mice were anaesthetized by intraperitoneal injection of 3.75 μl/g body weight of premixed (1:1) Hypnorm/Hypnovel (Hypnorm: Janssen Pharmaceutical, Belgium; Hypnovel: Hoffmann-La Roche Ltd, Switzerland). The lower hindlimbs were shaved, and the TA muscles injected with 2×10^9 vector genome of rAAVshDys-GFP (left TA) or rAAVshGL2-GFP (right TA) in 20–25 μl injectable saline (Sigma-Aldrich). Two or three mice were humanely killed at 9 days, and at 2, 4, 6, 9, 12, 15, 20, 24, 32 and 56 weeks after transduction. TAs were removed, mounted on cork discs in OCT embedding medium (Raymond A Lamb, Eastbourne, UK) and frozen in isopentane cooled with liquid nitrogen.

TA muscle sectioning and immunohistochemistry

Mounted TAs were stored at −80°C and subjected to tissue sectioning of 10 μm thickness, using a Bright OTF 5000 cryostat (Bright Instruments, Huntingdon, UK). The tissue sections were placed on glass slides pre-treated with (3-aminopropyl)triethoxysilane (APES, Sigma-Aldrich) and were left to air dry. The sample slides then were transferred to −80°C prior to use. Immunohistochemistry was performed using the M.O.M. kit for peroxidase (Vector Laboratories, UK), as per the manufacturer's protocol.

Mouse monoclonal primary antibodies were used at the following dilutions: NCL-DYS2, 1:50; Utrophin antibody, 1:10; NCL-a-SG, 1:200; and NCL-b-DG, 1:200. Following diamino benzidine (DAB) staining, the samples were dehydrated by immersion in 100% ethanol and cleared by incubation in xylene for 10 min, before mounting using DPX mountant (BDH, UK).

For morphological analysis of stained tissue sections, digital images were captured with a camera and processed using SigmaScanPro image analysis software (Systat Software, Hounslow, UK).

Statistical analysis

Data are represented as the mean plus standard deviation. Differences between groups were determined using the Student *t*-test. Differences between single fibre area distributions were assessed using a χ^2 analysis.

SUPPLEMENTARY MATERIAL

Supplementary Material is available at HMG Online.

ACKNOWLEDGEMENTS

We would like to thank Drs D. Grimm and J. Kleinschmidt, Germany, for kindly providing pDP6r and Dr Duan, USA, for kindly providing pDD345.

Conflict of Interest statement. None declared.

FUNDING

This research work was funded by Muscular Dystrophy Campaign, UK. M.M.G.S. was a recipient of a scholarship from Ministry of Science, Research and Technology, Iran.

REFERENCES

1. Emery, A.E.H. (1993) *Duchenne Muscular Dystrophy. Oxford Monographs on Medical Genetics*, 2nd edn. Oxford University Press, Oxford, UK, pp. 392.
2. Muntoni, F., Torelli, S. and Ferlini, A. (2003) Dystrophin and mutations: one gene, several proteins, multiple phenotypes. *Lancet Neurol.*, **2**, 731–740.
3. Bulfield, G., Siller, W.G., Wight, P.A. and Moore, K.J. (1984) X chromosome-linked muscular dystrophy (*mdx*) in the mouse. *Proc. Natl Acad. Sci. USA*, **81**, 1189–1192.
4. Sicinski, P., Geng, Y., Ryder-Cook, A.S., Barnard, E.A., Darlison, M.G. and Barnard, P.J. (1989) The molecular basis of muscular dystrophy in the *mdx* mouse: a point mutation. *Science*, **244**, 1578–1580.
5. Hoffman, E.P., Brown, R.H., Jr and Kunkel, L.M. (1987) Dystrophin: the protein product of the Duchenne muscular dystrophy locus. *Cell*, **51**, 919–928.
6. Chamberlain, J.S., Corrado, K., Rafael, J.A., Cox, G.A., Hauser, M. and Lumeng, C. (1997) Interactions between dystrophin and the sarcolemma membrane. *Soc. Gen. Physiol. Ser.*, **52**, 19–29.
7. di Blasi, C., Morandi, L., Barresi, R., Blasevich, F., Cornelio, F. and Mora, M. (1996) Dystrophin-associated protein abnormalities in dystrophin-deficient muscle fibers from symptomatic and asymptomatic Duchenne/Becker muscular dystrophy carriers. *Acta Neuropathol. (Berl)*, **92**, 369–377.
8. Petrof, B.J. (2002) Molecular pathophysiology of myofiber injury in deficiencies of the dystrophin–glycoprotein complex. *Am. J. Phys. Med. Rehabil.*, **81**, S162–S174.
9. Blake, D.J., Weir, A., Newey, S.E. and Davies, K.E. (2002) Function and genetics of dystrophin and dystrophin-related proteins in muscle. *Physiol Rev.*, **82**, 291–329.
10. Deconinck, N. and Dan, B. (2007) Pathophysiology of Duchenne muscular dystrophy: current hypotheses. *Pediatr.Neurol.*, **36**, 1–7.
11. Niebroj-Dobosz, I., Fidzianska, A. and Hausmanowa-Petrusewicz, I. (2001) Controversies about the function of dystrophin in muscle. *Folia Neuropathol.*, **39**, 253–258.
12. Elbashir, S.M., Harborth, J., Lendeckel, W., Yalcin, A., Weber, K. and Tuschl, T. (2001) Duplexes of 21-nucleotide RNAs mediate RNA interference in cultured mammalian cells. *Nature*, **411**, 494–498.
13. Martin, S.E. and Caplen, N.J. (2007) Applications of RNA interference in mammalian systems. *Annu. Rev. Genomics Hum. Genet.*, **8**, 81–108.
14. Scherr, M. and Eder, M. (2007) Gene silencing by small regulatory RNAs in mammalian cells. *Cell Cycle*, **6**, 444–449.
15. Lee, Y., Jeon, K., Lee, J.T., Kim, S. and Kim, V.N. (2002) MicroRNA maturation: stepwise processing and subcellular localization. *EMBO J.*, **21**, 4663–4670.
16. Zeng, Y., Wagner, E.J. and Cullen, B.R. (2002) Both natural and designed micro RNAs can inhibit the expression of cognate mRNAs when expressed in human cells. *Mol. Cell*, **9**, 1327–1333.
17. McManus, M.T., Petersen, C.P., Haines, B.B., Chen, J. and Sharp, P.A. (2002) Gene silencing using micro-RNA designed hairpins. *RNA*, **8**, 842–850.
18. Herndon, C.A. and Fromm, L. (2007) Directing RNA interference specifically to differentiated muscle cells. *J. Muscle Res. Cell Motil.*, **28**, 11–17.
19. Magee, T.R., Artaza, J.N., Ferrini, M.G., Vernet, D., Zuniga, F.I., Cantini, L., Reisz-Porszasz, S., Rajfer, J. and Gonzalez-Cadavid, N.F. (2006) Myostatin short interfering hairpin RNA gene transfer increases skeletal muscle mass. *J. Gene Med.*, **8**, 1171–1181.
20. Dodd, A., Chambers, S.P. and Love, D.R. (2004) Short interfering RNA-mediated gene targeting in the zebrafish. *FEBS Lett.*, **561**, 89–93.
21. Tinsley, J.M., Blake, D.J., Roche, A., Fairbrother, U., Riss, J., Byth, B.C., Knight, A.E., Kendrick-Jones, J., Suthers, G.K. and Love, D.R. (1992) Primary structure of dystrophin-related protein. *Nature*, **360**, 591–593.

22. Jung, D., Yang, B., Meyer, J., Chamberlain, J.S. and Campbell, K.P. (1995) Identification and characterization of the dystrophin anchoring site on beta-dystroglycan. *J. Biol. Chem.*, **270**, 27305–27310.
23. Tanabe, Y., Esaki, K. and Nomura, T. (1986) Skeletal muscle pathology in X chromosome-linked muscular dystrophy (*mdx*) mouse. *Acta Neuropathol. (Berl)*, **69**, 91–95.
24. Ahmad, A., Brinson, M., Hodges, B.L., Chamberlain, J.S. and Amalfitano, A. (2000) *mdx* mice inducibly expressing dystrophin provide insights into the potential of gene therapy for Duchenne muscular dystrophy. *Hum. Mol. Genet.*, **9**, 2507–2515.
25. Blankinship, M.J., Gregorevic, P., Allen, J.M., Harper, S.Q., Harper, H., Halbert, C.L., Miller, D.A. and Chamberlain, J.S. (2004) Efficient transduction of skeletal muscle using vectors based on adeno-associated virus serotype 6. *Mol. Ther.*, **10**, 671–678.
26. Takemitsu, M., Ishiura, S., Koga, R., Kamakura, K., Arahata, K., Nonaka, I. and Sugita, H. (1991) Dystrophin-related protein in the fetal and denervated skeletal muscles of normal and *mdx* mice. *Biochem. Biophys. Res. Commun.*, **180**, 1179–1186.
27. Tanaka, H., Ishiguro, T., Eguchi, C., Saito, K. and Ozawa, E. (1991) Expression of a dystrophin-related protein associated with the skeletal muscle cell membrane. *Histochemistry*, **96**, 1–5.
28. Matsumura, K., Ervasti, J.M., Ohlendieck, K., Kahl, S.D. and Campbell, K.P. (1992) Association of dystrophin-related protein with dystrophin-associated proteins in *mdx* mouse muscle. *Nature*, **360**, 588–591.
29. Lambert, M., Chafey, P., Hugnot, J.P., Koulakoff, A., Berwald-Netter, Y., Billard, C., Morris, G.E., Kahn, A., Kaplan, J.C. and Gilgenkrantz, H. (1993) Expression of the transcripts initiated in the 62nd intron of the dystrophin gene. *Neuromuscul. Disord.*, **3**, 519–524.
30. Wertz, K. and Fuchtbauer, E.M. (1998) Dmd(mdx-beta geo): a new allele for the mouse dystrophin gene. *Dev. Dyn.*, **212**, 229–241.
31. Nonaka, I. (1998) Animal models of muscular dystrophies. *Lab. Anim. Sci.*, **48**, 8–17.
32. de Leon, M.B., Montanez, C., Gomez, P., Morales-Lazaro, S.L., Tapia-Ramirez, V., Valadez-Graham, V., Recillas-Targa, F., Yaffe, D., Nudel, U. and Cisneros, B. (2005) Dystrophin Dp71 expression is down-regulated during myogenesis: role of Sp1 and Sp3 on the Dp71 promoter activity. *J. Biol. Chem.*, **280**, 5290–5299.
33. Hugnot, J.P., Gilgenkrantz, H., Chafey, P., Lambert, M., Eveno, E., Kaplan, J.C. and Kahn, A. (1993) Expression of the dystrophin gene in cultured fibroblasts. *Biochem. Biophys. Res. Commun.*, **192**, 69–74.
34. Pastoret, C. and Sebille, A. (1995) *mdx* mice show progressive weakness and muscle deterioration with age. *J. Neurol. Sci.*, **129**, 97–105.
35. Coulton, G.R., Morgan, J.E., Partridge, T.A. and Sloper, J.C. (1988) The *mdx* mouse skeletal muscle myopathy: I. A histological, morphometric and biochemical investigation. *Neuropathol. Appl. Neurobiol.*, **14**, 53–70.
36. Karpati, G., Carpenter, S., Morris, G.E., Davies, K.E., Guerin, C. and Holland, P. (1993) Localization and quantitation of the chromosome 6-encoded dystrophin-related protein in normal and pathological human muscle. *J. Neuropathol. Exp. Neurol.*, **52**, 119–128.
37. Pons, F., Robert, A., Marini, J.F. and Leger, J.J. (1994) Does utrophin expression in muscles of *mdx* mice during postnatal development functionally compensate for dystrophin deficiency? *J. Neurol. Sci.*, **122**, 162–170.
38. Waheed, I., Gilbert, R., Nalbantoglu, J., Guibinga, G.H., Petrof, B.J. and Karpati, G. (2005) Factors associated with induced chronic inflammation in *mdx* skeletal muscle cause posttranslational stabilization and augmentation of extrasynaptic sarcolemmal utrophin. *Hum. Gene Ther.*, **16**, 489–501.
39. Grounds, M.D. (2008) Two-tiered hypotheses for Duchenne muscular dystrophy. *Cell Mol. Life Sci*. Eprint ahead of publication (DOI 10.1007/s00018-008-7574-8).
40. Sanes, J.R. and Lichtman, J.W. (1999) Development of the vertebrate neuromuscular junction. *Annu. Rev. Neurosci.*, **22**, 389–442.
41. Minatel, E., Neto, H.S. and Marques, M.J. (2003) Acetylcholine receptor distribution and synapse elimination at the developing neuromuscular junction of *mdx* mice. *Muscle Nerve*, **28**, 561–569.
42. Hughes, B.W., Kusner, L.L. and Kaminski, H.J. (2006) Molecular architecture of the neuromuscular junction. *Muscle Nerve*, **33**, 445–461.
43. Carre-Pierrat, M., Grisoni, K., Gieseler, K., Mariol, M.C., Martin, E., Jospin, M., Allard, B. and Segalat, L. (2006) The SLO-1 BK channel of *Caenorhabditis elegans* is critical for muscle function and is involved in dystrophin-dependent muscle dystrophy. *J. Mol. Biol.*, **358**, 387–395.
44. Cossu, G., Eusebi, F., Senni, M.I. and Molinaro, M. (1985) Increased endocytosis of acetylcholine receptors by dystrophic mouse myotubes in vitro. *Dev. Biol.*, **110**, 362–368.
45. Xu, R. and Salpeter, M.M. (1997) Acetylcholine receptors in innervated muscles of dystrophic *mdx* mice degrade as after denervation. *J. Neurosci.*, **17**, 8194–8200.
46. Kong, J. and Anderson, J.E. (1999) Dystrophin is required for organizing large acetylcholine receptor aggregates. *Brain Res.*, **839**, 298–304.
47. Marques, M.J., Taniguti, A.P., Minatel, E. and Neto, H.S. (2007) Nerve terminal contributes to acetylcholine receptor organization at the dystrophic neuromuscular junction of *mdx* mice. *Anat. Rec. (Hoboken.)*, **290**, 181–187.
48. Graham, I.R., Hill, V.J., Manoharan, M., Inamati, G.B. and Dickson, G. (2004) Towards a therapeutic inhibition of dystrophin exon 23 splicing in *mdx* mouse muscle induced by antisense oligoribonucleotides (splicomers): target sequence optimisation using oligonucleotide arrays. *J. Gene Med.*, **6**, 1149–1158.
49. Boden, D., Pusch, O., Lee, F., Tucker, L., Shank, P.R. and Ramratnam, B. (2003) Promoter choice affects the potency of HIV-1 specific RNA interference. *Nucleic Acids Res.*, **31**, 5033–5038.
50. Xia, H., Mao, Q., Paulson, H.L. and Davidson, B.L. (2002) siRNA-mediated gene silencing in vitro and in vivo. *Nat. Biotechnol.*, **20**, 1006–1010.
51. Xia, H., Mao, Q., Eliason, S.L., Harper, S.Q., Martins, I.H., Orr, H.T., Paulson, H.L., Yang, L., Kotin, R.M. and Davidson, B.L. (2004) RNAi suppresses polyglutamine-induced neurodegeneration in a model of spinocerebellar ataxia. *Nat. Med.*, **10**, 816–820.
52. He, T.C., Zhou, S., da Costa, L.T., Yu, J., Kinzler, K.W. and Vogelstein, B. (1998) A simplified system for generating recombinant adenoviruses. *Proc. Natl Acad. Sci. USA*, **95**, 2509–2514.
53. Grimm, D., Kay, M.A. and Kleinschmidt, J.A. (2003) Helper virus-free, optically controllable, and two-plasmid-based production of adeno-associated virus vectors of serotypes 1 to 6. *Mol. Ther.*, **7**, 839–850.
54. Liu, Y.L., Wagner, K., Robinson, N., Sabatino, D., Margaritis, P., Xiao, W. and Herzog, R.W. (2003) Optimized production of high-titer recombinant adeno-associated virus in roller bottles. *Biotechniques*, **34**, 184–189.
55. Hermens, W.T., ter Brake, O., Dijkhuizen, P.A., Sonnemans, M.A., Grimm, D., Kleinschmidt, J.A. and Verhaagen, J. (1999) Purification of recombinant adeno-associated virus by iodixanol gradient ultracentrifugation allows rapid and reproducible preparation of vector stocks for gene transfer in the nervous system. *Hum. Gene Ther.*, **10**, 1885–1891.
56. Grimm, D., Pandey, K., Nakai, H., Storm, T.A. and Kay, M.A. (2006) Liver transduction with recombinant adeno-associated virus is primarily restricted by capsid serotype not vector genotype. *J. Virol.*, **80**, 426–439.
57. Bowles, D.E., Rabinowitz, J.E. and Samulski, R.J. (2003) Marker rescue of adeno-associated virus (AAV) capsid mutants: a novel approach for chimeric AAV production. *J. Virol.*, **77**, 423–432.